Josephson currents in two dimensional mesoscopic ballistic conductors

Heida, Jan Peter

Chapter 1

Introduction

1.1 Superconductivity and Josephson currents

In 1911 Kamerlingh Onnes [1] discovered that close to absolute zero temperature mercury can conduct electrical current without any resistance. Mercury shares this remarkable property with a number of other materials. Almost half a century later, Bardeen, Cooper and Schrieffer [2] explained this so called superconductivity in terms of a macroscopic number of conductance electrons that condense in Cooper-pairs all in the same quantum state. This quantum state of a superconductor is described by the condensate wave function

$$\Psi = |\Psi| e^{i\phi_s} \tag{1.1}$$

where ϕ_s is the macroscopic quantum phase and $|\Psi|$ is a measure of the Cooper pair density. In 1962 Josephson [3] predicted that a supercurrent can flow through an oxide layer separating two superconductors. The magnitude of this *Josephson current* depends on the difference $\phi_1 - \phi_2$ between the phases of the two superconductors:

$$I_{Josephson} = I_c \sin(\phi_1 - \phi_2) \tag{1.2}$$

where I_c is its maximum value, the critical current, which depends on $|\Psi|$. In turn, the phase difference is related to the voltage V across the junction by the fundamental law:

$$\frac{\mathrm{d}}{\mathrm{d}t}(\phi_1 - \phi_2) = \frac{2e}{\hbar} V \tag{1.3}$$

For finite voltages this leads to supercurrents oscillating at a well determined frequency. Soon these predictions were extensively confirmed by experimental work. Moreover, it was shown that Josephson currents can also flow through superconductor-normal metal-superconductor (SNS) junctions as well as various other so called 'weak links'.

In this thesis we report on experiments on Josephson currents through a special type of SNS system where the normal metal is a *two dimensional mesoscopic ballistic conductor*, adjectives explained in this introductory chapter.

The Josephson current depends on the phase difference of the superconducting electrodes. The vehicle transporting this phase information and the electronic charge between the two superconducting electrodes are the electron waves in the normal metal. To do so, they have to traverse the junction phase coherently. This brings us in the field which studies quantum aspects of electronic transport, *mesoscopic physics*, on which we elaborate below after discussing Andreev reflection and two dimensional conductors.

1.2 Andreev reflection

First we need a mechanism to transfer the macroscopic quantum phase from the superconductor to the electrons in the normal metal. This mechanism is Andreev reflection [4]. It arises when a conduction electron in a normal metal hits a SN interface. The electron at the Fermi energy μ can not enter the superconductor because there are no single particle states in an energy window of $\mu \pm \Delta$ with Δ the superconductor energy gap. This energy Δ can be viewed, in a simplified picture, as the condensation energy of the Cooper pairs at the Fermi energy. On the other hand, owing to the small value of the potential, $\Delta \ll \mu$, the electron can not be reflected since its momentum remains almost unchanged. Andreev found that the electron can drag along another electron with opposite momentum into the superconductor. Together these form a Cooper pair while in the normal metal the 'dragged along' electron can be described as a hole. The hole is retroreflected *i.e.* its momentum is almost identical to the electron momentum so that it retraces the path of the incoming electron. In this process, the superconductor phase is transferred as the phase difference between the incoming electron and Andreev reflected hole. Conversely, holes Andreev reflect into electrons.

1.3 Two dimensional conductors

Before a discussion of mesoscopic physics, we consider two dimensional electron gases, the most widely used realization of mesoscopic conductors.

With Molecular Beam Epitaxy crystals of semiconductor material can be formed with otherwise unavailable purity and crystalline perfection. Moreover, heterostructures of different materials can be grown with aligned crystal structures at the interfaces. By inserting a layer with a conduction band energy below that of the adjoining materials a quantum well in which the electrons in the heterostructure are trapped is formed. If this quantum well is thin enough so that only one subband is occupied it hosts a two dimensional electron gas (2DEG). In this thesis we use the quantum well formed by a 15 nm InAs layer bounded by AlSb layers. A 2DEG with electronic density n_s is filled up to the Fermi energy

$$\mu = \hbar^2 k_F^2 / 2m \tag{1.4}$$

with m the effective electron mass and k_F the Fermi wave vector

$$k_F = \sqrt{2\pi n_s} \tag{1.5}$$

The properties of 2DEGs make them very well suited for mesoscopic physics. A number of them are:

1. Owing to their low electron density n_s, the Fermi wavelength $\lambda_F = 2\pi/k_F$ is rather large. In our samples $\lambda_F \approx 17$ nm.

2. They have a circular Fermi surface so that at the Fermi energy the electron waves $e^{ik_F x}$ have the same Fermi wave vector k_F in all directions.

3. The matching of crystals assures clean interfaces so that the 2DEG has a high electron mobility, and electron mean free paths l_{el} up to 10 μm can be achieved.

4. Long electron-phonon and electron-electron scattering times assure a long inelastic scattering length l_{in}. For our samples we estimate $l_{in} \approx 10$ μm.

5. The electron density can be regulated, and even depleted with the application of an electric field in the direction perpendicular to the 2DEG. This field can be applied with gates on top of the host material.

6. The density of states $\rho(E) = 2m/2\pi\hbar^2$, with m the effective electron mass, is independent of energy. This simplifies the effects of excursions from the Fermi energy, such as in SNS systems where electrons from an energy range of a few times Δ around the Fermi energy affect the electron transport.

1.4 Mesoscopic Physics

We now take some time to elucidate the field of *mesoscopic physics*. For electronic transport, this term is in general use when the quantum mechanical nature of the electrons has a profound influence on a samples conductance [1]. This influence is described by coherent interferences of electron waves. Thus, mesoscopic phenomena take place over length scales shorter than the phase coherence length l_ϕ. This length is bounded by for instance the inelastic scattering length. Elastic scattering does not modify phase coherence, so that quantum effects of electron interference can be observed in both ballistic and diffusive systems. With ballistic we mean that the system size L is smaller than the electron mean free path l_{el}. It can now be seen that the properties of 2DEGs in semiconductor heterostructures along with modern lithographic methods by which sample sizes down to 50 nm can be made, make it possible to realise mesoscopic samples and even ballistic mesoscopic samples.

However, we still need low temperatures to study mesoscopic phenomena. First of all because at low temperatures the inelastic electron scattering length is large. Secondly because phase coherence is lost due to thermal smearing in the following way: After a time τ, two electrons following the same path with energy difference δE acquire a relative phase difference of $\tau\delta E/\hbar$. If $\tau\delta E/\hbar = \mathcal{O}(1)$, these electrons are uncorrelated, and so is their quantum interference. In the time τ these electrons travel a length of $v_F\tau \approx \hbar v_F/\delta E$ in a ballistic system, and $\sqrt{D\tau} \approx \sqrt{\hbar D/\delta E}$ in a diffusive system with diffusion constant D. For electrons at a temperature T distributed according to the Fermi-Dirac function, the energy difference $\delta E \approx k_B T$ so that the thermal coherence length is

$$\xi_{T,b} = \hbar v_F/k_B T \tag{1.6}$$

for ballistic systems while it is

$$\xi_{T,d} = \sqrt{\hbar D/k_B T} \tag{1.7}$$

for diffusive systems. Hence, only at sufficiently low temperatures the correlation can be maintained.

We now present a few selected topics from mesoscopic physics. Comprehension of these topics will aid in understanding later chapters on the Josephson current in two dimensional mesoscopic ballistic conductors. A review of mesoscopic physics is given by Beenakker and van Houten in Ref.[5].

[1] More general, mesoscopic physics studies the physical effects between microscopic and macroscopic scales. From the Greek; mikros = small, mesos = medium, makros = large.

1.4.1 Conductance quantization

Two 2DEG regions can be separated by a ballistic quantum point contact which is a short and narrow ballistic constriction with a width W of the order of the Fermi wavelength: $W \approx \lambda_F \ll l_{el}$. This can be realised by depleting the 2DEG of electrons using a split gate, or etching isolated channels in the 2DEG as schematically shown in Fig.1.1. Such a quantum point contact constitutes a potential well for the electrons in the 2DEG; when only one subband of this potential well is filled it is a 1D system. Each subband is generally referred to as a *mode*. The number of modes for a square potential well is

$$N = \mathrm{int}\left[\frac{k_F W}{\pi}\right] \tag{1.8}$$

van Wees *et al.* [6] and Wharam *et al.* [7] independently discovered that the conductance through quantum point contacts is quantized in units of $2e^2/h \approx (13\ \mathrm{k}\Omega)^{-1}$. The quantum conductance is e^2/h per transmission channel, the factor of 2 arises from spin degeneracy of the electrons. It is found, that each mode contributes $2e^2/h$ to the conductance so that the total conductance is

$$G = N\frac{2e^2}{h} \tag{1.9}$$

Their ballisticity assures that backscattering processes play no role in the conductance through quantum point contacts. With increasing point contact width, the energy separation between the modes becomes very small and the quantum effects are smeared. In this regime the conductance is the so called Sharvin conductance for a ballistic 2D constriction [8]:

$$G_{Sharvin} = \frac{2e^2}{h}\frac{k_F W}{\pi} \tag{1.10}$$

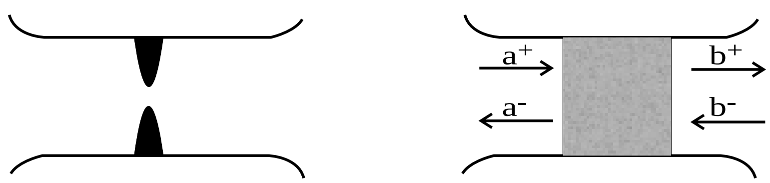

Figure 1.1: Left: A quantum point contact separating two 2DEG regions. Right: A diffusive region separating two contacts. The arrows schematically indicate the incoming and outgoing partial waves (see text)

1.4.2 Landauer approach to conduction

Whereas for ballistic systems each mode n has a probability $T_n = 1$ to cross the sample, in a diffusive system backscattering from the diffusive region occurs. Also, an electron wave from the source in mode n can arrive at the drain in a different mode m. A system of ideal leads coupled by a diffusive region is shown in Fig.1.1.

A wave incident on the diffusive region is built up of partial waves in all modes, and can be described as a vector

$$c^{in} = (a_1^+, a_2^+, \ldots, a_N^+, b_1^-, b_2^-, \ldots, b_N^-) \tag{1.11}$$

where a_i^+ and b_i^- are the amplitudes of the partial waves in mode i in the right and left direction respectively. Thus the incoming wave is $\Psi(x) = \sum_{i=1}^{N}[a_i^+ \exp(ik_i x) + b_i^- \exp(-ik_i x)]$. Similarly outgoing waves are described by the vector

$$c^{out} = (a_1^-, a_2^-, \ldots, a_N^-, b_1^+, b_2^+, \ldots, b_N^+) \tag{1.12}$$

These vectors are related by the scattering matrix S via $c^{out} = Sc^{in}$ with

$$S = \begin{pmatrix} r & t' \\ t & r' \end{pmatrix} \tag{1.13}$$

Here r and r' are $N \times N$ matrices of reflection probability amplitudes and t and t' are $N \times N$ matrices of transmission probability amplitudes. The element t_{nm} of t is the probability amplitude for a (partial) wave in the incoming mode n to be transmitted into the outgoing mode m. To satisfy current conservation S is a unitary matrix. The eigenvalues $\mathcal{T}_i$ of the matrix $tt^\dagger$ fully determine the conductance which, for the linear response regime, leads to:

$$G = \frac{2e^2}{h} \sum_{i=1}^{N} \mathcal{T}_i \tag{1.14}$$

This formula is known as the Landauer formula [9]. By looking at the eigenmatrix of $tt^\dagger$ the problem is simplified, it is now the problem of a region with decoupled transmission channels each characterised by a transmission probability $\mathcal{T}_i$. These transmission channels are a linear superposition of all modes. For a ballistic system the transmission channels are simply the modes, $tt^\dagger$ is already an eigenmatrix, and all transmission probabilities are unity which leads to Eq.1.9.

1.4.3 Weak localization

In diffusive media there is a set of trajectories which return an electron to the place where it started from. These closed loops can be traversed clockwise or counter clockwise, with probability amplitudes A_l and A_r respectively. From time reversal symmetry $A_l = A_r = A$. Classically the probability of backscattering via such a pair of trajectories is $P_{cl.} = |A_l|^2 + |A_r|^2 = 2|A|^2$ *i.e.* the sum of the probabilities of both trajectories. Quantum mechanically however we have to sum the amplitudes first so that the probability becomes $P_{q.m.} = |A_l + A_r|^2 = |A_r|^2 + |A_l|^2 + 2|A_r A_l| = 4|A|^2$ *i.e.* double the value of the classical probability. This enhanced backscattering, known as *weak localization*, leads to a decrease in the conductance of a diffusive sample with respect to the classical result. All trajectories with a length shorter than the phase coherence length contribute. With decreasing temperature, more and more trajectories contribute so that the conductance decreases with decreasing temperature. A magnetic field breaks time reversal symmetry ($A_l \neq A_r$) and lifts weak localization. For samples with a width W and length L the correction on the conductance is of order $(e^2/h)(W/L)$.

1.4.4 Universal Conductance Fluctuations

Classically, a sample can be thought as built up of q uncorrelated segments each having a conductance G_q. The average conductance $<G>$ is then qG_q while the variance

$$\mathrm{Var}(G) = \sqrt{<(G- <G>)^2>} \tag{1.15}$$

is $\sqrt{q}G_q$ which rapidly becomes smaller than $<G>$ with increasing q. Consequently, for classical systems sample to sample fluctuations in the conductance can be ignored. For fully phase coherent diffusive wires with

$$l_{el} \ll W \ll L \ll l_\phi \tag{1.16}$$

however, quantum interference leads to significant sample to sample fluctuations with a remarkable property:

$$\mathrm{Var}(G) \approx \frac{e^2}{h} \tag{1.17}$$

i.e. $\mathrm{Var}(G)$ is of the order of the quantum conductance e^2/h regardless of the sample size and the degree of disorder as long as Eq.1.16 is satisfied. Therefore these fluctuations are termed Universal Conductance Fluctuations (UCF). They arise from quantum interference of electron waves which sense the entire sample. Although two samples may have identical average conductance $<G>$ the potential landscape, and thus the unique interference pattern which determines the conductance, can be different. If Eq.1.16 is not satisfied there are L/l_ϕ sections (assuming $W \ll l_\phi$ is satisfied) that fluctuate independently which reduces amplitude of the fluctuations.

Mathematically an ensemble of samples with the same average conductance $< G >$ can be described as a set of random t matrices with the same average properties. The transmission eigenvalues $\mathcal{T}_n$ of such random matrices have a bimodal distribution, most of them are exponentially small while a few transmission channels have near unity transmission. A fundamental property of these matrices is that taking another member of the ensemble, *i.e.* changing the sample interference pattern, creates on average an extra opened or closed transmission channel. Since the conductance of such a channel is $2e^2/h$, this leads to UCF.

UCF can be observed in a single sample; one does not need to physically rearrange the impurities. One way to change the interference pattern is via the dynamical phase $\tau E/\hbar$ an electron at energy E picks up after travelling a time τ. The conductances at E and $E + E_c$ are uncorrelated if $\tau E_c/\hbar = \mathcal{O}(1)$. This energy E_c is called the correlation energy. For the conduction electrons, the energy E is the Fermi energy $\mu = \hbar^2 \pi n_s/m$ which can be controlled via the electron density n_s with the use of a gate. By changing the Fermi energy with E_c, we effectively create a new sample. In general $E_c \ll \mu$ so that the average properties are not affected. Another way to modify the interference pattern is the application of a magnetic field B. The vector potential $\vec{A}$ acts on the phase θ an electron picks up travelling a certain path via $\theta = \int_{path} \vec{A} \mathrm{d}\vec{l}$. Uncorrelated situations are separated by a correlation field B_c which is the field where one flux quantum $\Phi_0 = h/e$ is added to the flux $\Phi = BWL$ penetrating the sample.

UCF is a sample specific property, the magnetoconductance for instance is a unique property of each individual sample, set by the impurity configuration. The universal nature appears in the statistical properties of the magnetoconductance.

1.4.5 Summary

By discussing a number of mesoscopic phenomena, we have introduced some widely used concepts from mesoscopic physics. These concepts such as the Landauer approach to conduction, the influence of a magnetic field, the dynamical phase electrons acquire along their path and the influence of temperature on phase coherence, will play an important role in later chapters.

1.5 Scope of this thesis

In this thesis, the fields of Josephson currents and mesoscopic physics are combined. With the presented experiments we address the question: *'How does the Josephson current pass through a two dimensional mesoscopic ballistic conductor and what are its properties ?'*

The widely accepted theoretical description of supercurrents in mesoscopic Josephson junctions is that of supercurrent carrying bound states as first published by Kulik [10]. These bound states are formed by electron wave functions that interfere with themselves after two Andreev reflections. This theoretical framework is presented in Chapter 3. Normally bound states form on a length scale comparable to the Fermi wavelength from the condition $k_F L = n\pi$ with $n = 1, 2, 3, \ldots$. In SNS systems however bound states can be formed on larger length scales because the Andreev reflected hole cancels the dynamical phase picked up by the electron. This process, called phase conjugation is also discussed in Chapter 3.

As mentioned the theoretical answer to the above raised question is *'via supercurrent carrying bound states'*. We may thus also phrase our question as *'Do we observe supercurrent carrying bound states, and if so, what are their properties ?'*.

To find an answer we first need to appreciate the phenomena of electronic transport through Josephson junctions. This knowledge is summarized in Chapter 2. The used InAs quantum wells with which our samples are made are discussed in Chapter 4 along with the fabrication and characterisation of the samples, and we introduce the concept of diffusive Andreev reflection resulting from extra scattering introduced by the cleaning procedure of the InAs surface prior to deposition of the superconductor electrode.

The observed critical current magnitude and its temperature dependence are discussed in Chapter 5. The critical currents found from experiments on mesoscopic Josephson junctions are in general an order of magnitude smaller than theoretical predictions. We argue that these predictions are made for over-idealised samples and do not cover the experimental situation. In this Chapter, we hypothesize on the effect of diffusive Andreev reflection on the supercurrent carrying bound states. Also the magnetic field dependence of the critical current in the used samples differs from known theories for idealised systems as shown in Chapter 6. In fact we find that current theory is inadequate to describe the found periodicity of I_c in a small magnetic field. We present a heuristic approach to explain the observed results. An extension to higher magnetic fields is studied in Chapter 7.

Whereas the above deals with the zero bias critical current of the junctions, in Chapter 8 we study the current-voltage characteristics of our junctions. The finite voltage behaviour is the result of a complicated interplay of the Josephson frequency and sample specific time scales of multiple Andreev reflection and inelastic scattering.

In Chapter 9 we address the issue of bound states via the normal conduction in a region around them which is expected to depend on the phase difference between the superconducting electrodes.

Finally, we added Chapter 10 although it is a bit out of the scope of the main topic of this thesis. It reports our work on gate-controlled spin-orbit scattering in a 2DEG which drew our attention while characterising a similar heterostructure as used for the mesoscopic Josephson junctions.

References

[1] H. Kamerlingh Onnes, Akad. van Wetenschappen (Amsterdam) **14**, 818 (1911).

[2] J. Bardeen, L. N. Cooper, and J. R. Schrieffer, Phys. Rev. **108**, 1175 (1957).

[3] B. D. Josephson, Phys. Lett. **1**, 251 (1962).

[4] A. F. Andreev, Zh. Eksp, Teor. Fiz. **46**, 1823 (1964), [Sov. Phys. JETP **19**, 1228 (1964)].

[5] C. W. J. Beenakker and H. van Houten, in *Solid State Physics Volume 44*, edited by F. Seitz, D. Turnbull, and H. Ehrenreich (Academic Press Inc., New York, 1991).

[6] B. J. van Wees *et al.*, Phys. Rev. Lett. **60**, 848 (1988).

[7] D. A. Wharam *et al.*, J. Phys. C **21**, L209 (1988).

[8] Y. V. Sharvin, Zh. Eksp. Teor. Fiz. **48**, 984 (1965), [Sov. Phys. JETP **21**, 655 (1965)].

[9] R. Landauer, IBM J. Res. Dev. **1**, 223 (1957).

[10] I. O. Kulik, Zh. Eksp. Teor. Fiz. **57**, 1745 (1969), [Sov. Phys. JETP **30**, 944 (1970)].